spaceR: Knitting Ready-Made, Tactile, and Highly Responsive Spacer-Fabric Force Sensors for Continuous Input

Roland Aigner
Mira Alida Haberfellner
roland.aigner@fh-hagenberg.at
mira.haberfellner@fh-hagenberg.at
Media Interaction Lab, University of Applied Sciences Upper Austria
Hagenberg, Austria

Michael Haller
michael.haller@unibz.it
Free University of Bolzano-Bozen
Bolzano-Bozen, Italy

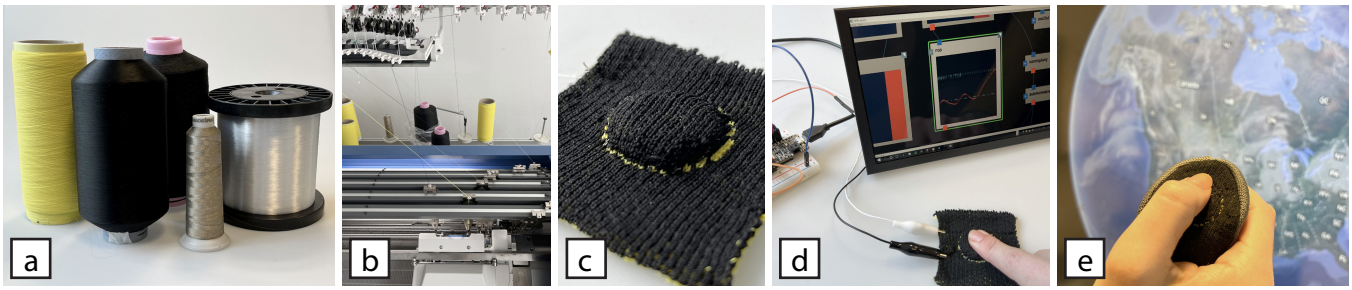

Figure 1: Five yarn materials (a) are combined in a weft knitting process (b) to create a compressible textile UI element (c). It is highly sensitive to pressure and enables for precise, continuous input (d). It can furthermore be extended to more complex elements that provide more sophisticated input modalities, such as fully-knitted, drapable 4-way controllers (e).

ABSTRACT

With spaceR, we present both design and implementation of a resistive force-sensor based on a spacer fabric knit. Due to its softness and elasticity, our sensor provides an appealing haptic experience. It enables continuous input with high precision due to its innate haptic feedback and can be manufactured ready-made on a regular two-bed weft knitting machine, without requiring further post-processing steps. For our multi-component knit, we add resistive yarn to the filler material, in order to achieve a highly sensitive and responsive pressure sensing textile. Sensor resistance drops by ~90% when actuated with moderate finger pressure of 2 N, making the sensor accessible also for straightforward readout electronics. We discuss related manufacturing parameters and their effect on shape and electrical characteristics and explore design opportunities to harness visual and tactile affordances. Finally, we demonstrate several application scenarios by implementing diverse spaceR variations, including analog rocker- and four-way directional buttons, and show the possibility of mode-switching by tracking temporal data.

UIST '22, October 29-November 2, 2022, Bend, OR, USA

ACM ISBN 978-1-4503-9320-1/22/10.
https://doi.org/10.1145/3526113.3545694

CCS CONCEPTS

• **Human-centered computing** → **Interaction devices**; Haptic devices; *Interaction techniques.*

KEYWORDS

knitting, spacer fabric, pressure sensor, resistive sensor, textile interface, e-textiles

ACM Reference Format:
Roland Aigner, Mira Alida Haberfellner, and Michael Haller. 2022. spaceR: Knitting Ready-Made, Tactile, and Highly Responsive Spacer-Fabric Force Sensors for Continuous Input. In *The 35th Annual ACM Symposium on User Interface Software and Technology (UIST '22), October 29-November 2, 2022, Bend, OR, USA.* ACM, New York, NY, USA, 15 pages. https://doi.org/10.1145/3526113.3545694

1 INTRODUCTION

We currently see ongoing miniaturization of electronics and devices, along with advances in material science [8] and improved accessibility of manufacturing machinery [29] paving the way to a world of smart and networked devices. This trend amplifies opportunities for sensors and interaction interfaces embedded in textiles [7], not only in specialized garments [34], but also in furniture upholstery, vehicle interior, etc. While state-of-the-art solutions, e.g., in car seats, are often printed devices that are hidden away, we noticed an increasing demand for innovative all-in-one solutions in recent years. This is to save manufacturing costs and assembly effort, but also for creating more lightweight solutions, that are simultaneously more durable and less error-prone, as well as easy to replicate and replace. Related to this are also considerations

regarding sustainability and recycling [53]. This trend is also eminent from revelations like the award-winning Bosch Sensor Glove[1], or the MIT 3D Knit BioSuit prototype[2] recently presented at the 2022 MARS conference, both of which underline the power and versatility of cutting-edge knitting technology and its potential for assembling resilient functional textiles by combining highly specialized materials.

Currently, there is considerable effort in R&D towards a seamless integration of user interfaces into textiles, both in research [38] and in industry. However, many current solutions suffer from disadvantages of different kinds. Capactive sensing of touch on deformable and stretchable objects is inherently challenging [1]; also, shielding from external influences is difficult, especially for traces linking the sensors to electronics. For resistive sensing on the other hand, the canonical approach requires a stacked, multi-layer solution [54], which reduces flexibility and increases complexity in labor and composition. Other solutions suffer from design issues like being hardly recognizable as UI elements [38] and/or missing self-explanatory affordances [36].

In this paper, we present spaceR, an implementation of resistive pressure sensing in a multi-component spacer fabric that is clearly perceptible by a distinct bulge and provides pleasant haptic properties (cf. Figure 1c). Building upon a study from Mlakar et al. [31], we utilize a convex cross-section profile, that is not only recognizable by visual but also by tactile means and passively informs about functionality [30], in that it affords to be pressed. The spacer fabric is soft and easily compressible by up to ~90%, depending on manufacturing parameters. It is highly sensitive to pressure, and enables for continuous and precise control of a scalar value. The choice for resistive based sensing allows for operation with straightforward sampling electronics and operation without skin-touch, e.g., when wearing gloves. Even though we focus on usage as a UI element in this paper, it can be easily applied in entirely different sensing scenarios.

spaceR is created from a minimum of 5 yarns and can be fabricated on a regular computer-controlled two-bed weft knitting machine, which gives great flexibility to control several design aspects and intricate details on loop-level, including but not limited to position, size, shape, and functionality. Filler material in the spacer fabric induces haptic feedback that is controllable at design-time, and provides a tactile experience similar to foams, yet in contrast, the procedure of weft knitting does not produce cutoff waste. Unlike other textile manufacturing solutions, such as multi-step augmentation of pre-existing fabrics [2], our spacer fabric sensors are created in a single manufacturing step, ready for use.

In summary, the contributions of this paper are the following:

- A method for implementing localized spacer fabric pressure sensor elements within a surrounding textile, which support continuous (i.e., non-binary) input, and provide comfortable haptic properties and feedback due to the fabric's elasticity.
- We list insights and manufacturing details for knitting our spacer sensors, including an in-depth evaluation of the elements' performance metrics and encouraging results of a small-scale washing-test.
- We present a design space related to manufacturing opportunities and discuss respective potentials.
- We demonstrate the feasibility of our sensors as versatile UI elements by incorporating them into generic knit structures, and show diverse use cases highlighting the sensor's expressiveness when used as a UI element, ranging from single-buttons, over utilization of temporal data, to implementations of multiple sensitive regions within a single element.
- Finally, we include knitting instruction files in Knitout format in the supplementary material that can be used to replicate our results.

2 RELATED WORK

Soft and deformable interfaces are of high interest in both industry and research for a variety of application domains, including soft robotics, locomotion [21], actuation [10, 20], healthcare monitoring [8, 22, 50], and interaction devices in general [24, 41], as they tend to provide pleasant haptical properties and natural feedback when deformed. Many works deal with inflatable objects [10, 13], elastomers [25, 44] with potential of integrating sensoric within the actuators [6], or used multi-component printing to create deformable and reconfigurable meta-material sensors [14]. Many other have used textiles, which are generally perceived as comfortable on the skin, due to their appealing properties of breathability, flexibility, and potential elasticity.

Textile-based interfaces have been of interest in the research community for a long time. A notable seminal work in HCI was the Musical Jacket [34], presented in 1998 by Orth et al., it was however in the last decade that textiles gained more momentum in the HCI community. Concepts for sensing on fabrics have been explored and developed for a huge variety of applications [7, 33, 38, 48], with sensing techniques including capacitive [16, 37, 48], resistive [2, 18], and inductive [15] methods, and combinations thereof [46, 52]. Applied textile manufacturing methods include weaving [38], knitting [26], as well as sewing [49] and embroidery [1] of pre-existing fabric.

Especially knitting has recently gained traction in this field. As modern flatbed knitting machines are getting more accessible and workflows are greatly simplified [19, 29, 32], they find their way also into well-equipped maker spaces. In academic research, recent work [4, 43] investigated knit strain sensors incorporating a single conductive yarn; Barabina et al. present in [5] a knit pressure sensor using different materials for sensor and connector traces, which is closer to our approach. 3DKnITS also uses multi-component pressure-sensitive knits[3]. We extend these ideas in that we embed our sensors in a spacer fabric structure, which provides high compressibility and is discoverable also by purely tactile means.

Printed resistive-based force sensors have been in use for decades [12] and can be replicated relatively easily with textiles by stacking multiple layers. This approach has been translated to textile by

[1] https://www.textiletechnology.net/technical-textiles/trendreports/Technical-Textiles-32020-Knitted-sensor-glove-22011

[2] https://www.media.mit.edu/posts/dava-newman-presents-3d-knit-biosuit-at-mars-conference/

[3] https://www.media.mit.edu/projects/3dknits

Rofouei et al. [39], who introduced a smart textile consisting of an array of pressure sensors, by sandwiching a resistive textile in between of two conductive layers. Numerous related projects employ this method, including SmartMat [47], eCushion [54], SimpleSkin [9], and Tapis Magique[4]. To increase softness, DIY designers extended this idea by adding foam layers in between[5]. In contrast, we are able to avoid a multi-layered approach by knitting a multi-component sensor, that is ready for use without requiring any further manufacturing steps.

Researchers have in the past presented spacer fabric structures with sensing ability, mostly using highly conductive yarn on both faces [42]. Vu et al. [50] developed a capacitive pressure sensor for gloves and furthermore integrated them into socks for gait analysis. In the HCI field, Albaugh et al. [3] demonstrated a spacer fabric augmented with conductive yarn to enable capacitive sensing of touch and hover. Choi et al. [11] performed an in-depth analysis of pressure sensors on warp knitted spacer fabrics, implemented with Ag-coated conductive yarn, which showed very low electrical resistance. Our design uses different materials with vastly different conductance values for clearly separating sensing and connecting areas, for making the sensor reading agnostic to actuation along the connector traces.

Honnet et al. presented a method for in-situ polymerization with Polypyrrole [17], in order to turn arbitrary materials, such as foams and textiles, into highly responsive resistive sensors. Similarly, Kim et al. [23] introduced a pressure sensor by carbon nanotube ink drop-coating a pre-existing spacer fabric. However, the isolated treatment of exclusive object sub-parts seems to be difficult in both cases. Even though there are experiments with selective treatment of only parts of the fabrics, reproducibility depends on careful handling and requires tedious manual labor. Our approach offers precise control on loop-level, easy customization and great variability in terms of sensitive sub-area positions, shapes, surface geometries, and tactile properties, by selectively knitting resistive parts. Once designed, identical knits can be easily replicated.

3 PREREQUISITES

3.1 Operational Principle

Our spacer sensor's functionality is based on the widespread force sensitive resistor (FSR) [12]. In a common implementation of an FSR, a piezoresistive layer is sandwiched between two electrodes[6], where surfaces are in relatively loose contact at rest. Whenever pressure is applied, the materials are more densely compressed, causing a drop in electrical resistance (see Figure 2), which is termed the *Interface Effect* [51]. We utilize this simple idea and translate it to spacer fabrics in that we substitute resistive film by resistive yarn and printed electrodes by conductive yarn. In the following, we elaborate on the design of our spacer sensors which can be knit in a single piece using a computer-controlled v-bed weft knitting machine with at least four yarn carriers (in its most simple form) and two needle beds.

[4]https://www.media.mit.edu/projects/tapis-magique/
[5]https://www.kobakant.at/DIY/?p=48
[6]Arguably the most widespread implementation places two interdigitated electrodes on-top of the resistive layer

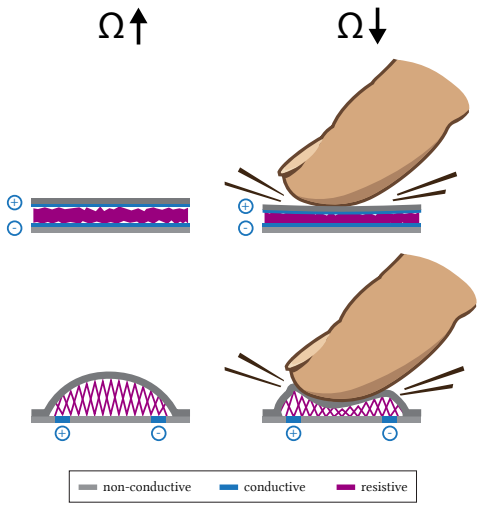

Figure 2: When printed force sensors are compressed, the contact area between electrodes and piezoresistive film rise, causing a drop in electrical resistance (top). We translate this to spacer knits by knitting a compressible resistive filler, that acts as a variable resistor in between two highly conductive traces (bottom).

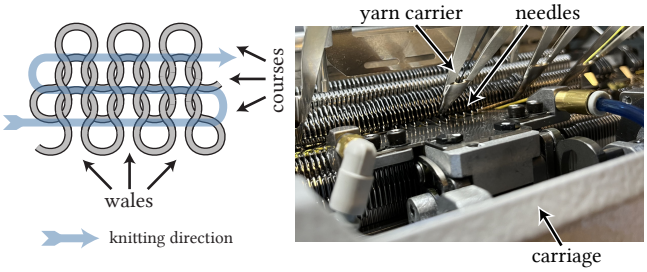

Figure 3: Structure of a basic knit (left) and closeup of main components of a weft-knitting machine (right).

3.2 Weft Knitting Basics

A weft knitting machine consists of a carriage that moves along the bed, pushing and pulling needles via a machine-operated cam. One or more yarn carriers move along the carriage, in order to feed yarn to the extending needle hooks. The result of this process is a fabric that is gradually built from bottom to top in a row-major fabrication direction (cf. Figure 3). According to this process, the shapes and patterns that can be accomplished are limited and their complexity largely depends on the number of a machine's yarn carriers and the operations a needle can perform. The following list provides terminology that is required within the context of this paper. For further details, we refer to [29, 45].

Courses and wales: rows and columns in a knit, respectively.
Knit stitch: forms a new loop. A needle is extended and clears the currently held loop. The yarn carrier guides the yarn

through needle's hook. The pulling-back of the needle encloses the yarn by means of a closing latch and pulls it through the currently held loop(s).

Tuck stitch: inlays additional yarn into a needle hook. Similar to knitting, except the currently held loop is not cleared and stays in the hook, with the new yarn added.

Float stitch: passes the yarn behind a needle. The needle is not extended and therefore, the yarn does not interact with it.

Plying: two or more yarn ends are placed in the same carrier. As a result, both yarns are taking the exact same path in the fabric and cannot be separated in the knitting process.

Plating: each yarn is placed in an individual carrier, however the carriers feed the same needles, sequentially. In contrast to plying, the programmer has loop-level control on exactly where multiple yarns are combined and which yarn is front.

Stitch size: the length of a loop results from the magnitude of the needles' pulling-back during the knit-stitch process (see above). The effective loop length affects the fabric's tightness and is a result of the programmable stitch size (aka. stitch number) setting, as well as on other factors, such as manually adjusted yarn tension, the yarn's material, and optional finishing steps. The nominal stitch size can be controlled on needle-level by the programmable cam, however frequent changes can seriously decrease manufacturing speed.

3.3 Spacer Fabric Anatomy

Even though the manufacturing process takes place on a flat bed, the result can be of elaborate three-dimensional shape [32]. The term "3D-knit" generally refers to fabrics of relatively complex geometry that are ready-made by sophisticated knitting procedures and machinery, without requiring any cutting and sewing of pieces. However, 3D-knits could be considered 2.5D-knits constituting certain surface shapes and need to be distinguished from spacer fabrics, that constitute actual *volumetric* knits, initially developed to replace toxic laminated-layer foam [45]. Spacers are knit structures incorporating rather stiff monofilament filler material, that is inlaid between two opposing knit faces, in order to fill up volume and provide elasticity (cf. Figure 4c). Depending on filler material and thickness, as well as finishing steps, such as thermal activation, the resulting fabric can be of high (e.g., for shock absorbers in protective gear) or low stability (e.g., for a replacement of foams in upholstery). In contrast to 3D-knits, spacers' surfaces can just as well be planar.

In a spacer fabric, the monofilament filler is alternately tucked into loops of both beds. When the fabric leaves the machine, the faces shrink due to inherent elasticity, which causes the filler filaments to rise and therefore to push both faces apart. This principle is illustrated in Figure 4d; note that h is constant due to the nylon material. For manufacturing parameters, we refer to the terminology used by Albaugh et al. [3] (cf. Figure 5):

Filler tuck spacing: the distance between front and back tuck of the filler yarn pattern, specified in number of needles.

Filler row density: ratio of filler to face-pair courses inserted. E.g., a density of 3/1 would specify three inserted filler courses per one pair of front/back face course.

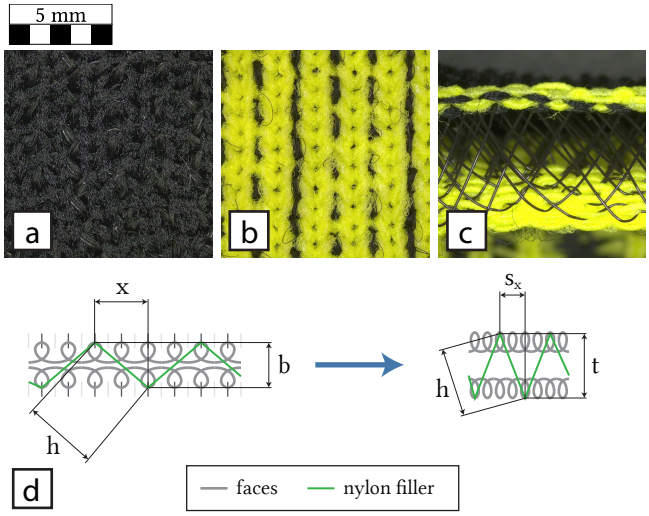

Figure 4: Closeup of a spacer fabric structure: front face (a), back face (b), and cross-section with nylon filament filler (c). Fabric shrinkage when coming off the needle beds, in combination with the nylon's stiffness (h remains constant), causes the nylon filler to erect and push both faces apart (d).

Tuck pattern offset: the course-directional shift of the tuck pattern for each inserted filler row, specified in number of needles. In our work, positive values shift in right direction.

For manufacturing spaceR elements, we use relatively thin filament to achieve soft and elastic fabrics, that are easily deformable and provide comfortable haptic properties. Furthermore, we want to be able to control resulting thickness and elastic behavior. As discussed by Albaugh et al. [3], the spacer thickness is mostly subject to the filler's *tuck spacing* and the *shrinkage* of the knit faces, which is the lateral draw-in caused by the material's elasticity. This causality is intuitive since the theoretical maximum thickness is achieved when the filler strands are completely orthogonal to the faces (cf. Figure 4d). Albaugh et al. stated the equation

$$t = \sqrt{x^2 + b^2 - s_x^2} \tag{1}$$

to estimate the thickness that would result from a tuck distance during knitting x, in a machine with bed distance b and tuck distance within the shrunk fabric s_x. Note that x has to be a multiple of the fixed needle distance (i.e., of neighboring needles on a single bed) and b is non-variable since it is the fixed distance of opposing needles of the machine's front and back beds. Hence, we can infer from Equation 1 that the achievable thickness rises with increasing x and decreasing s_x. Note that shrinkage is in practice limited, depending on the yarn material(s) in use. According to commercial knitters within our professional network, inherent shrinkage can be facilitated by plying Spandex together with the base material, reinforcing nylon filaments to rise.

4 DESIGN & MANUFACTURING

4.1 Basic Design

Basing our sensor's functionality on the principle of an FSR, we combine the filler with resistive yarn in order to yield a piezo-resistive compressible volume. When at rest, the filler structure provides a high resistance, however when compressed, the number of contacts increases, and the overall resistance drops (cf. Figure 2), therefore our design principle utilizes the interface effect.

As a substitute of the FSR's electrodes, we knit two traces of conductive yarn at opposite ends of the pressure sensitive volume, for connecting the sensor with external electronics at a remote part of the textile, e.g., using crocodile clamps for laboratory usage. The combination of high- and low-resistance yarns serves the purpose of increasing the resistance ratio of sensing part and connecting part. This is crucial for making the senor agnostic to deformations on the connector traces, which would otherwise introduce significant glitches in the sensor readings.

To facilitate fabric shrinkage, we knit at half-gauge (i.e., only using every second needle on the machine's beds) and used 100% Spandex on the back face: to allow the forming of a distinct bulge, we found it essential to use Spandex on one face only. Otherwise the opposing forces on both faces contracted the filler too much which yielded poor results. Expectedly, fully shifting the shrinking agent to the back bed increased the fabric's curling tendency. As a positive side-effect, this clears the front bed for arbitrary materials and their combinations, which enables to design visual and haptic properties more freely. Specifically, the materials used were:

Polyamide (PA) as non-elastic base material for knitting front faces. We plied two ends with dimension of dtex 78/17/2 from TWD Fibres GmbH.

Spandex as a contracting yarn for the back faces. We combined two cones of wrapped spandex threads (covered yarn with 1× dtex 395 PA core + 2× dtex 44/13/1 PA spandex wrap) from Meya Grabher-Meyer GmbH.

Nylon for the monofilament filler material. We tried diameters of ø=0.17 mm, ø=0.12 mm, and ø=0.1 mm. Based on our own preference, we settled on plying two ends of ø=0.07 mm + ø=0.1 mm, both plied in a single carrier. We found this combination resulted in more pleasant haptics and appealing response when pressed, as compared to single strands that would correspond to similar amount of filler.

Resistive yarn as an inlay along the nylon, at force sensitive areas. We plied three ends of Resistat P6204 Merge H100i from Shakespeare Conductive Fibers LLC[7], which is a den 100/24 (dtex 111/24) bicomponent Polyester yarn with a conductive sheath and average linear resistance of 1.5 MΩ/cm, according to specification.

Conductive yarn for knitted connectors traces. We used Madeira HC40[8] silver plated Polyamide yarn with dtex 290 and linear resistance of <300 Ω/m, according to specification.

[7]https://shakespeare-pf.com/product/polyester/
[8]https://shop.madeira.co.uk/hc-40-2500m-cone-(high-conductive)_hc40-xxx-xxx.htm

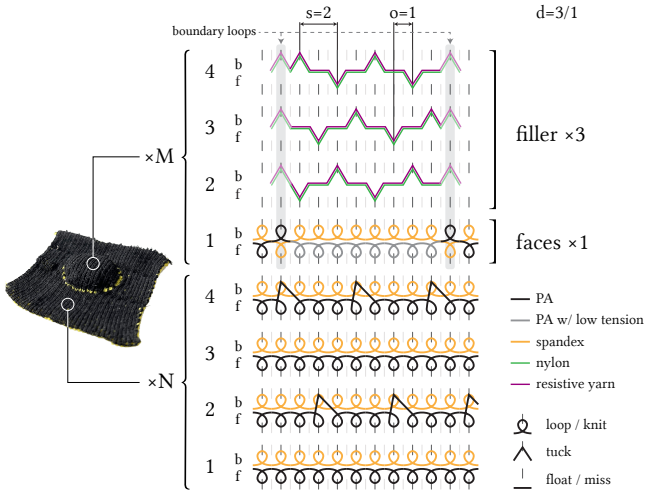

Figure 5: Knitting pattern of our spaceR elements (bottom to top). We knit N repetitions of the depicted 4-course surrounding structure, with front and back faces connected by tucking. Within the spacer region, we tuck the filler front and back, alternatingly, with a tuck spacing of s needles. The tuck pattern is offset by o needles for every filler course. In this example, we tuck 3 courses of filler per 1 course of front/back faces, hence density d = 3/1. The filler inlay is additionally tucked at the boundary regions of the spacer element (wales shaded in grey). We knit at half-gauge, so every other needle is idle.

4.2 Implementation

For our first samples, we incorporated circular spacer buttons into surrounding non-spacer knits, i.e., the filler was only inserted within the boundaries of this circular regions. *Front and back faces* were plain knits, which were at off-button areas connected by tucking front to back face at every 4th wale on every other course, with a 2-wale offset each (cf. Figure 5). Furthermore, as recommended in [3], we alternated the order of knitting front and back courses, to reduce filler shearing effects. For sake of simplicity, we performed this not only within the button-area, but throughout the whole textile.

Within button boundaries, we increased the stitch size of the front face to enforce the filler to push this area outwards. We inserted nylon and Resistat as a filler by plating them with two carriers.

At boundary loops, we interlocked front and back yarn to get a distinctly outlined shape, i.e., we knit the front yarn to the back bed and vice versa. Since we used high-contrast yarn colors for front and back faces, we also established a visual outline in doing so.

Additionally, we tucked the filler to the back bed at those boundary loops, to hold it in place, since we would otherwise risk it getting pulled out of previous needles when performing the turnaround for the subsequent course. We furthermore increased the stitch size of the Polyamide yarn within the button area significantly to cause an imbalance in the faces' yielding to filler pressure, and therefore facilitate the creation of a bulge on this side of the fabric (cf. Figure 1c). For further implementation details, we refer to the Knitout files

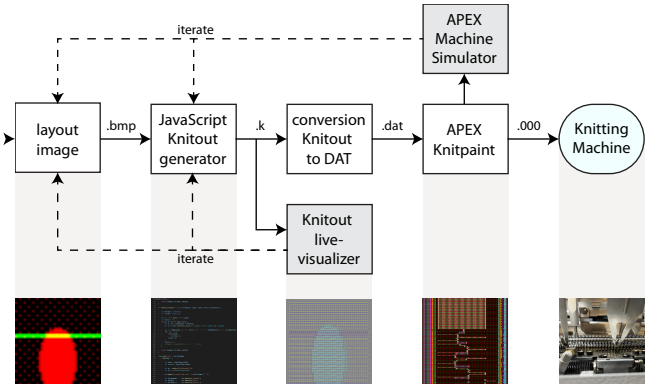

Figure 6: Our pipeline consists of a custom JavaScript based conversion from bitmap files to Knitout, which enables quick iteration by editing images with basic drawing applications.

in the supplementary material. Knitting speed was set to 0.5 m/s for all face yarns and 0.3 m/s for the filler, since more consistent results were achieved when inserting the filler with lower speeds.

4.3 Parameters and Variations

All samples presented in this work were knit on a 15-gauge Shima Seiki SWG061N_2 with APEX4 software suite (version S-04.C), at half-gauge. Since during our early exploration phase we had to fabricate numerous variations, we used a specialized development-pipeline (cf. Figure 6) to speed up iteration time. Most central is that we used the Knitout high-level knit description language [28] as an intermediate format. Knitout is a human-readable knit program description that greatly simplifies manual edits and quick visual verification using the associated tools [55]. Since the format is text-based, it is straightforward to create programs and scripts that generate Knitout files.

We started from bitmap-image files, encoding different structural regions on the fabric as pixel colors, which enabled us to quickly draw different layouts and patterns using basic drawing programs. Via a custom JavaScript and the according Knitout frontend[9], we generated Knitout instructions from those images for potential corrections by manually edits, and for visual verification in the knit schematic using the *Knitout (Live) Visualizer*[10]. We then converted Knitout files to target DAT format that could be opened in Shima Seiki KnitPaint for knitting simulation and generation of the binary machine-program files. All Knitout source files used for this work can be found in the supplementary material.

5 EVALUATION

Albaugh et al. discuss in [3] the effects of several spacer fabric manufacturing parameters on mechanical properties. We chose to vary these for our spaceR sensors and observe how they affect the appearance as well as haptic and technical characteristics of the resulting element. Varied parameters and their ranges were the following:

filler tuck spacing: As discussed, tuck spacing has a major impact on the achieved thickness; we inherently expect considerable influence on the button travel distance (i.e., compressibility) and therefore on the element's fidelity. We varied tuck spacing values between 2, 3, and 4 for our evaluation samples.

filler row density: We also expect filler row density to be a crucial factor since adding more filler may promote the pressing apart of font and back faces. Additionally, it may also reinforce firmness, which would be noticeable during actuation. We included filler row density variations of of 2/1, 3/1, and 4/1.

stitch size: As discussed, we increased the front face's (Polyamide) loop lengths within the sensing area in order to amplify the creation of a distinct bulge. We anticipate that different loop lengths will elicit different results; while low stitch sizes will keep the filler from extending, high stitch sizes are expected to have an opposite affect. Additionally, we may even see an effect on the height profile. We tried stitch sizes ranging from borderline low to reasonably high, as determined empirically. Settings on the machine were 20/10, 24/14, 28/18, and 32/22 for S/LS[11], respectively. Stitch settings were uniform 30/20 for the back face spandex, and 25/15 for the Madeira connector traces.

We started from a circular button and chose as a baseline a combination of parameters that we judged to yield acceptable results during our initial exploration phase, which were spacing of 3, density of 3/1, and stitch size of 24/14.

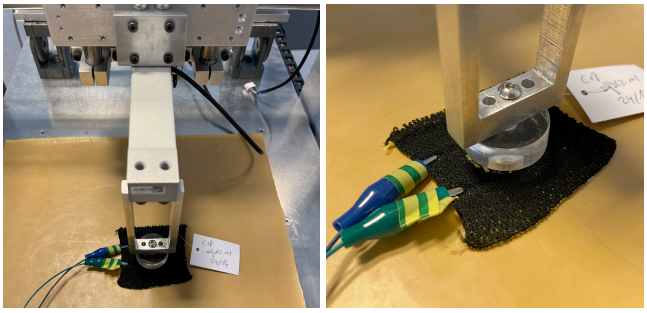

Figure 7: Our automated tester machine is equipped with a force cell (left) to record precise actuation, along with measurements of sensor resistance (right).

5.1 Apparatus

For a technical characterization of our buttons' performance regarding pressure, we modified a custom-built CNC router to a pressure-tester (cf. Figure 7). The machine was controlled by ArtSoft Mach4 CNC Control Software (v4.2.0), running on a Windows 10 PC. The actuator mount features a single-point load-cell of type

[9]https://github.com/textiles-lab/knitout-frontend-js
[10]https://textiles-lab.github.io/knitout-live-visualizer/, Github repository: https://github.com/textiles-lab/knitout-live-visualizer

[11]S = stitch, LS = leading stitch settings of the programmable cam, that are represented in abstract numbers and do not have correlation to physical values, according to Shima Seiki.

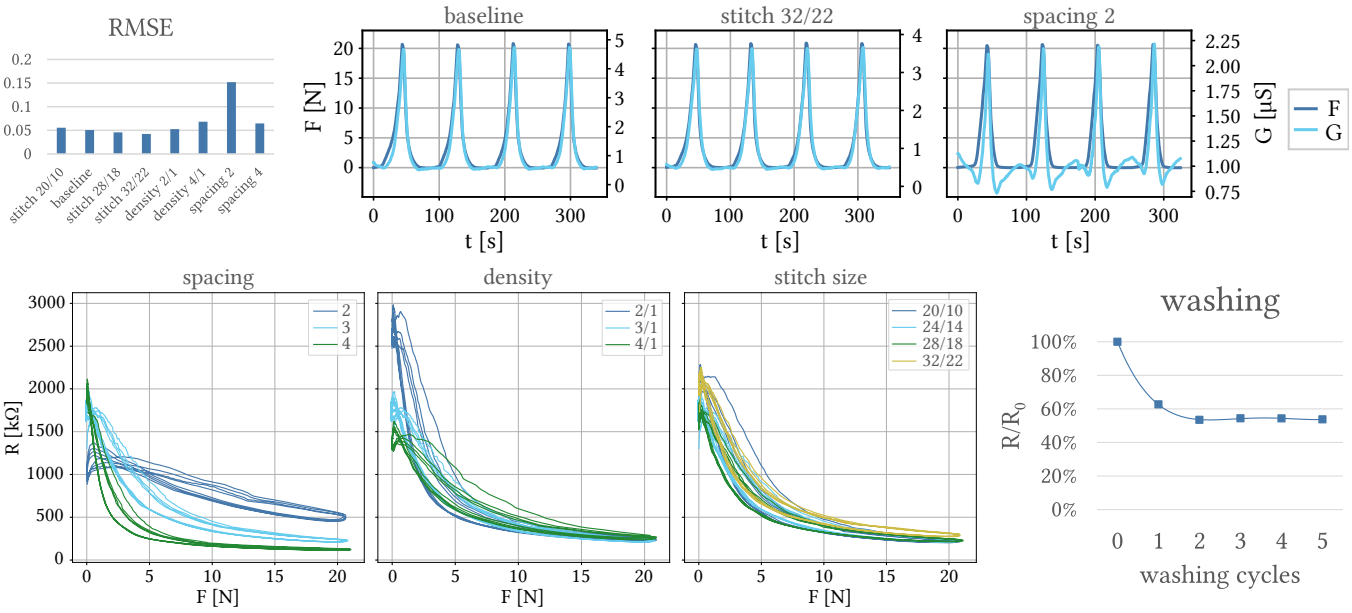

Figure 8: Top: Overlays of force F and conductivity G on timelines (top) show a striking conformity between actuation and sensor reading in most of our knit samples. We present the timelines of our baseline sensor, along with the best and worst performing variations. Bottom: Force-to-resistance characteristics lines show little hysteresis. Sensors with highest spacing values (center, green) reach saturation rather quickly. Preliminary washing tests hint towards a settling of resistance values after the 2nd to 3rd washing cycle.

Sauter CP P1-Ba-d-1810[12], which was sampled by an ADS 1231 24-bit Delta-Sigma ADC[13] at 80 Hz. Sampling and data collection were performed with an Adafruit ESP32, which also communicated with Mach4 via RS232, in order to control the CNC router's test procedure according to measured actuation of the textile. The sensor's electrical resistance was sampled by the same ESP32, using a simple voltage divide with reference resistance of 606 kΩ and an Adafruit ADS1115 16-bit ADC[14] at 128 Hz. Sample data including force, resistance, actuator displacement along Z, and timestamp were stored into a CSV file for subsequent analysis. Jog speed along Z-axis was ~0.15 mm/s, we therefore logged at a relatively low rate of ~10 Hz.

We placed the fabric samples on rubber sheets (1.5 mm) and secured them with double-sided tape, to keep it completely flat. We then connected the measurement electronics with crocodile clips to the knit connector traces. Using a circular actuator with ø=30 mm, we repeatedly increased the applied force up to 20 N (~28.3 kPa), which we estimated representative for a relatively strong finger press, and after dwelling for one second, returned the actuator back to its starting position using identical jog speed. Recorded raw data can be found in the supplementary material.

In a small-scale experiment, we also tested our baseline sensor against the effects of washing, applying the procedure suggested in [40]. Together with 1 kg of carrier fabric, we washed five times at 40°C in an AEG Lavamat Protex with a water volume of 7 l. We used neutral soap at 1% by weight and washed for 35 minutes. The spin program was 2 minutes at 800 rpm, followed by 5 minutes at 1000 rpm; rinsing was done for 3 minutes at 20°C with 7 l of water. After each washing cycle, the sensors were air dried for 3 hours at 24°C and 35% relative humidity. We then measured with a UNI-T UT61B digital multimeter, and noted resistance values after allowing for 20 s of settling.

5.2 Results and Discussion

In Figure 9 we see an overview of the effects of manufacturing parameters to the sensor performance. As for the sensors' absolute resistance values at rest, varying filler spacing has the greatest effect with an increase of 86% when increased from 2 and 4. Increasing filler density from 2/1 to 4/1 on the other hand decreases resistance by 49%. Changing front face stitch size had a non-consistent and comparably low effect, with the greatest variation of 22% when decreasing tightness from 28/18 to 32/22.

Varying filler spacing seems to have the most striking effect to the dynamic range, which we defined as

$$\text{dnr} = \frac{\overline{R}_0 - \overline{R}_f}{\overline{R}_0},$$

where $\overline{R}_0$ and $\overline{R}_f$ are the mean resistances at rest and at full actuation, respectively. While the button with filler spacing of 2 showed a considerable dynamic range of 55% already, those with spacing 3 and 4 were by far superior with 88% and 94%. Filler density had a moderate effect, almost linearly decreasing the dynamic range by 9% when moving from density 2/1 to 4/1. Varying front face stitch

[12] https://www.sauter.eu/cgi-bin/cosmoshop/lshop.cgi?action=showdetail&ls=en&rubnum=produkte.263.309&artnum=CP-P1|-|-|309
[13] https://www.ti.com/product/ADS1231
[14] https://www.adafruit.com/product/1085

Figure 9: Sensors' absolute resistance values are shown on top, where $\overline{R}_0$ and $\overline{R}_f$ are mean values at rest and at full actuation, respectively. Filler density had a noticeable effect, while stitch size for front face loops had minor impact. Varying filler tuck spacing affects sensor dynamic range the most (bottom).

size had only a slight effect. Tighter knit button area (20/10) resulted in highest range of 90%, while our sample with lowest tightness showed 86%. We infer that there is great flexibility in modifying manufacturing parameters, without affecting the resulting sensor quality much, with the exception of spacing, which should be reasonably high. We value this a comfortable finding, since it is also in unison with advantageous haptic qualities.

The relation of measured force and resistance in Figure 8 also show that varying tuck spacing and filler density has greatest effect on the sensors' characteristics. The higher the spacing value is chosen, the sooner the sensors reach saturation. However, for our lowest chosen spacing value of 2, we can see erratic behavior at low forces. This also stands out in the timeline plots, where we found mostly striking alignment between applied force F and sensor conductivity G, however the variation with filler spacing of 2 stands out with distinct overshooting at actuation and release and severe settling effects at the low-force regions. This hints to the internal structure moving and re-arranging after pressure was removed. We calculated RMSE between F and G for each sensor, from values normalized to a range of [0 1][15]. Again, the results (cf. Figure 8) show that most variants perform exceptionally well in that regard, with the exception of the sample with spacing of 2.

The results of our washing tests suggested that there is reasonable electrical and outstandig mechanical durability. Although the resting resistance dropped considerably during the first two washing cycles, it settled at ~54% of the initial value with negligible change throughout another 3 washing cycles. We did not notice any visual signs of damage or abrasion after a total of 5 washing cycles. Comparing the results to other sensors, e.g. as presented in [5], we hypothesise this is due to the sensing part being enclosed in surrounding structure, which could provide protection to some degree. Moreover, it was unexpected to see the resistance drop instead of rise, however, we refrained from a more detailed analysis at this point. Most interestingly, even though the absolute values dropped, the sensor's dynamic range was only slightly affected, as we still calculated a dynamic range of 82% (pre-washing: 88%), which means the functionality of the sensor remained nearly unaffected.

[15]We calculated mean G and mean F at rest and at full load, and mapped those ranges to [0 1].

6 DESIGN EXPLORATION & APPLICATION EXAMPLES

For applying our sensors in a real-world scenario, we explored potential modifications, extensions, and use case scenarios in an interdisciplinary focus group, consisting of professional UX-designers, textile designers, HCI scientists, and computer scientists. Within a timeframe of three weeks, we manufactured numerous functional and non-functional prototypes and identified several benefits. First, since it is possible to create convex and concave surfaces, our elements can be designed as tactile interfaces for eyes-free interaction. Furthermore, we noticed our ability to control several attributes that are valuable from an UX design perspective. In the following, we elaborate on our experiments and findings.

6.1 Design Considerations

Inspired by a user study on UI design parameters for textile user interfaces by Mlakar et al. [31], we systematically explored several directions we found relevant in such scenarios. We formulated a design space (cf. Figure 10) and reflected on the impact of the elements' tactile characteristics and overall performance. In particular, we present our experiments and findings regarding the spacer's active area *size*, its *thickness*, its outline *shape*, its *cross-section profile*, and its tactile reaction to pressure, i.e., its *firmness*. Note that most of these factors will certainly be inter-dependent, to some degree.

6.1.1 Size. As shown in [31], the element's size is a valuable design parameter. It can be utilized for eyes-free element identification and, most notably, it can provide intuitive association of UI elements to body parts. E.g., huge buttons would be operated with the palm, big ones with the thumb, tiny ones with the pinkie. Therefore, size can be applied in UI design to afford correct hand placement and posture. We expected size to have an impact on obtainable thickness and also on resulting height profile, since the interlocking of front and back faces at the element edge loops restrict the filler's ability to erect. Consequently, we expected this to have side-effects on technical aspects like button travel distance and dynamic range. We experimented with three different circular buttons of ø=17 mm, ø=25 mm, and ø=40 mm (all manufacturing parameters were kept constant). The results confirmed a great impact of area size on achievable height (cf. Figure 12). As expected, smaller areas seem to progressively frustrate the establishing of volume. However, since there is a physical limitation for the nylon filler to erect, we expect this interference is hardly noticeable beyond a certain size, which is also hinted by a tendency to converge, slight visible in the chart.

6.1.2 Thickness. To find correlations between spacer thickness and manufacturing variables, we measured the height of the buttons we created for our technical evaluation. In Figure 12, we see that filler spacing has an immense effect on resulting thickness. Within our parameter range of 2 thru 4, we see almost linear correlation, which is in line with the findings in [3]. Increasing density seems to have a very minor opposite effect; within our limited testing range it also appears to be linear. Varying stitch size for front faces within the button area also gives an expected result: within the

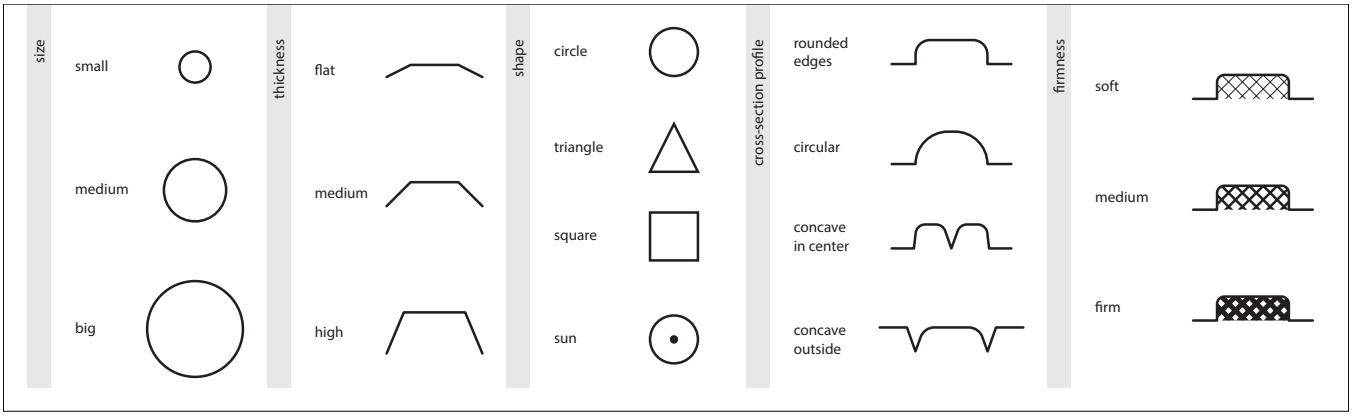

Figure 10: We explored a design-space within a focus-group, experimenting with different sizes, thickness, shapes, cross-section profiles, and degrees of firmness.

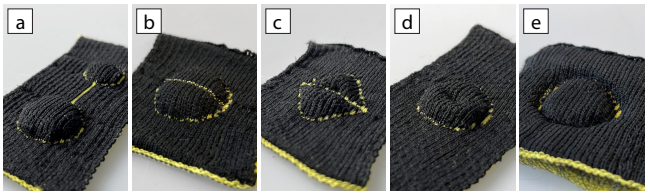

Figure 11: Our exploration phase resulted in several design variations, including dual buttons, combining different sizes, which are connected to one interface union by visual and haptic means (a), rocker-buttons with separate pressure sensitive segments for *up/down*, with visual (b) and tactile separations (c), buttons with concave regions for affording finger alignment at the center (d), and elements that were embedded in a surrounding spacer fabric and identifiable by concave edges (e).

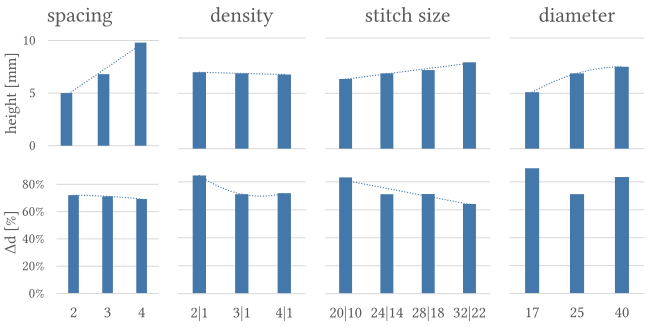

Figure 12: In line with related work, spacer element height can be mostly controlled by varying filler tuck spacing. Button compressability, depends mostly on filler density and front face stitch size, but is also affected by the elements diameter, i.e., by its area size.

samples that were knit with less tension, the filler seems to be less constricted and therefore a higher bulge can be achieved.

6.1.3 Shape. Using our pipeline that enabled us to draw the basic layout in a bitmap image, it was straightforward to experiment with different outline shapes, such as ellipses, triangles, squares, and diamonds (cf. Figure 11c). From our experience with those basic geometric primitives, we did not observe notable limitations, however, more complex ones, e.g., outlines including concave regions on top and/or bottom, could be challenging due to the course-major working process of weft knitting. Apart from this intrinsic limitation, we see great opportunities in freedom of design.

6.1.4 Cross-Section Profile. During preliminary experiments, we noticed a capability of controlling the shape of the spacer's cross-section, since we observed some were more edged than others. In Figure 13, we present the traced cross-sections of the buttons we created for our evaluation. We can see that filler density did not change the profile dramatically, while spacing had a vast impact. Most interestingly, changing loop length showed an effect on edge angularity; stitch size setting of 32/22 established an almost rectangular profile.

6.1.5 Firmness. We designed our buttons specifically to achieve a comparably soft and uniform pressure response, by plying two ends of particularly thin nylon monofilaments, choosing relatively high filler density, and balancing against the amount of Resistat we had to use to still get reasonable conductivity. As a result, we do not get the pressure characteristics that are distinct for regular spacer fabrics. Most spacer structures resist more strongly until the nylon filaments tilt at a certain force, which depends on the material's stiffness. In contrast, our buttons require only little force to compress from the very beginning. We calculated the effects of our manufacturing parameters to relative travel distances of the buttons we created with

$$\Delta d = \frac{\overline{t_0} - \overline{t_f}}{\overline{t_0}},$$

where $\overline{t_0}$ and $\overline{t_f}$ are mean thickness at rest and full actuation, respectively. Figure 12 shows that lower tuck spacing resulted in higher travel distance. Reducing filler density had a similar effect, just as reducing loop length. Tactile properties are inherently subjective,

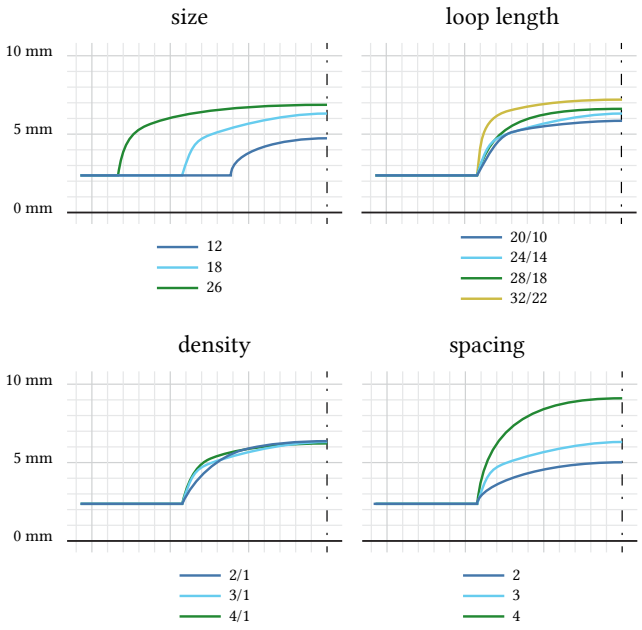

Figure 13: The cross-section profiles of our spaceR samples differ, depending on shape and manufacturing parameters and can be designed accordingly.

however we judged the haptic appeal of our initial ply of two ends with ø=0.07 mm + ø=0.1 mm superior to thicker monofilaments, that produce more firm results.

6.2 Applications

In the following section, we present a number of application scenarios that show the benefits of our spacer sensor. They demonstrate the continuous input sensing capability and high sensitivity. Furthermore, users are enabled to adjust and control pressure according to perceived haptic feedback.

For all demo applications, we used Adafruit HUZZAH32 ESP32 Feather Boards[16] in combination with simple voltage dividers, with reference resistors of 330 kΩ for the lower-resistance 4-way controller and 606 kΩ for all others. To avoid crosstalk between voltage dividers, we separated the voltage sources by providing 3.3V individually, using different DACs as output pins. We sequentially measured each sensor, providing power by setting the respective DAC to HIGH while letting the others float. We multisampled at max speed with the ESP's on-board 12-bit ADCs and averaged ~15 samples before moving to the next sensor, resulting in an overall sample rate of ~400 sps. Samples were sent to a custom application on a Windows PC via USB, for further processing and utilization. Our data processing pipeline required only trivial techniques such as background-subtraction, high- and low-pass, etc., and combinations thereof. The processed data was then forwarded via OSC protocol to demo applications created with C++ and Unity3D. For a schematic and more details about the used processing pipeline we refer the interested reader to the supplementary material.

[16] https://www.adafruit.com/product/3405

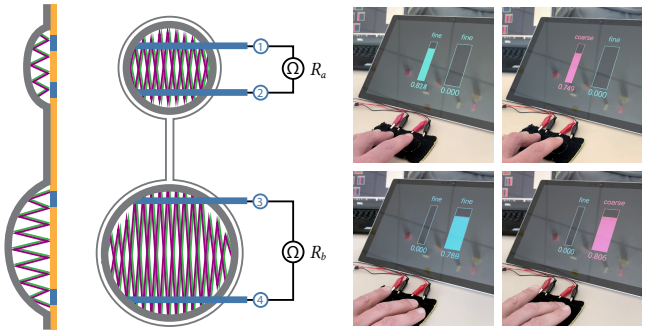

Figure 14: In our dual-button implementation, we combine two isolated buttons of different size on a single fabric, each of which has its own connector traces. We analyze temporal input to add a second input modality, which enables mode switching.

6.2.1 Multi-Functional Dual-Button. We combined two spacer buttons of different sizes (ø=20 mm and ø=28 mm with thickness of 5.7 mm and 8.6 mm, resp.) in a single textile patch (cf. Figure 14) and associated them visually by interlocking front and back loops along two wales in the center (cf. Figure 11a). This associating line also provides a tactile clue for locating the counterpart button for eyes-free interaction, while button sizes can be used to hint towards a respective function, e.g., increase/decrease. Furthermore, we can harness the buttons' responsiveness to utilize temporal data, and use a high-pass filter to implement mode switches, i.e., change to a different input mode if the sensor reading changes quickly. In our application, we demonstrate its performance by controlling a shutter (cf. Figure 17a) with two functions: the implementation maps the buttons to mode *shutter up/down* when pressed quickly, and to *tilt forwards/backwards* when pressed gently.

6.2.2 Up/Down Rocker-Button. Beyond simple buttons, we see great potential for designing more complex control elements, with multiple independent active parts integrated in a single element. By introducing a centered, course-directional separation on a symmetrical element, we create a hint towards dichotomous functions of the respective halves, similar to the style of a common rocker-button. This can be done purely visually, but also by shaping the depth profile to give a tactile clue (cf. Figure 11b and c). One advantage of the latter is the possibility to center the finger entirely from tactile sensation. To achieve the separating concave line, we knit one course with interlocked pattern (cf. Figure 15), connecting front and back faces across the whole spacer element. By cutting the filler in between, we electrically separate the sensor structure into two parts, each of which are equipped with individual pairs of conductive traces on the back face. The result is a two-way controller, that enables natural up/down input by slight tilting motions and can be easily controlled in a continuous manner, e.g., for adjusting scrolling speed (cf. Figure 17b). For amplifying the directional character of the sampled data, we found it beneficial to apply the signal difference in our applications, i.e., $y = s_y(R_{down} - R_{up})$, with s_y being a constant scaling factor for mapping values to a normalized range.

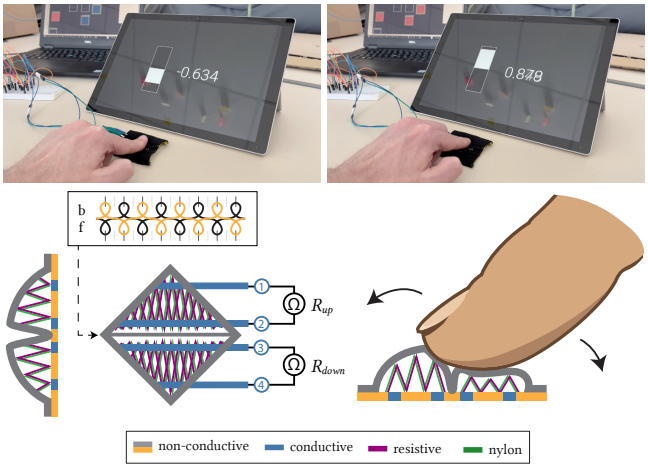

Figure 15: The implementation of a rocker-button for continuous control of *up/down* is accomplished by separating the filler into two separate regions within a single element. Each sub-section is provided with a pair of connectors. The convex separating notch is realized by interlocking loops along one course. The result provides control with intuitive tilt gestures.

6.2.3 4-Way Controller. Pushing the complexity of our structure, we designed a 4-way controller, with a layout similar to a d-pad. Due to the continuous sensing capabilities, the input modality is close to that of a thumbstick. By interlocking 2×2 loops in the center, we create a tactile reference point for natural placement of the finger at the origin (cf. Figure 11d). From there, tilting motions in either direction causes pressure on the embedded active areas, which act as individual analog buttons. We incorporated separate pressure-sensitive areas in one single spacer element, by cutting the plied resistive yarn in between, knitting parts solely with nylon filler, resulting in isolated active areas (cf. Figure 16). For sake of simplicity and due to the risk of manufacturing flaws within the limited filler volume, we chose not to separate responsive areas for left and right. Instead, we use one shared pressure sensitive area in the center, and separated one of the connector traces instead, in order to measure left and right ends respectively. Due to this shared sensing area, applied pressure on the left would slightly affect readings on the right and vice versa. We countered this in signal processing, by again utilizing differential values, as we did in our implementation of the rocker-button. We therefore calculated the controller's x-axes with $x = s_x(R_l - R_r)$ and $y = s_y(R_d - R_u)$ using s_x and s_y again as constant scaling factors. For our use cases, this simple solution proved to be adequate. Note that it is indeed possible to completely separate left from right resistive areas when using an additional yarn carrier for adding a second plated part with resistive yarn in the same courses, however it is more challenging from a manufacturing point of view. For testing our sensor as an input device replacing a thumbstick, we simulated a virtual gamepad via vJoy [17] for controlling games and other applications such was Google Earth.

[17] https://github.com/jshafer817/vJoy

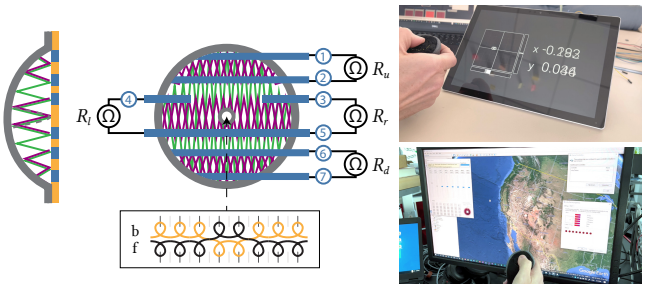

Figure 16: Our design of a 4-way controller features a convex dent in the center, for easy alignment of the finger. We implemented a navigation control for Google Earth to demonstrate continuous 4-way input in a single spaceR element.

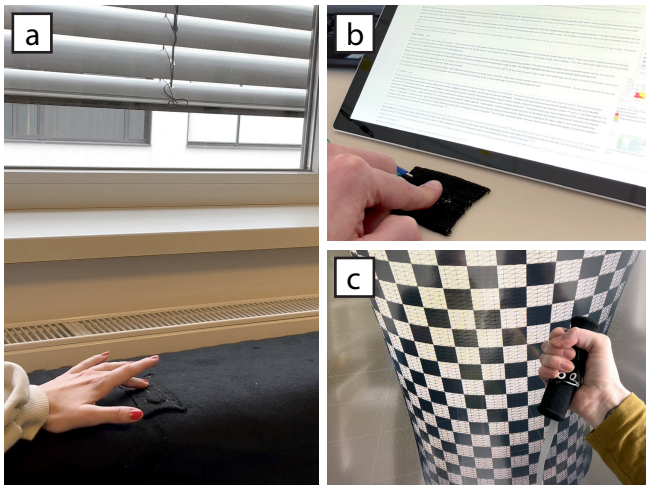

Figure 17: Our application scenarios for spaceR variations included a shutter control (a), controlling bi-directional scrolling speed of a webpage (b), and a visualization of a cylinder, deformable by localized squeezing (c).

6.2.4 Squeeze Controller. As a rather experimental user interface, we implemented an improvised squeeze controller (cf. Figure 17c) with four separate buttons on a single knit that we wrapped around a bicycle handle foam. The buttons were similar in layout to the ones we created for the Dual-Button, however oval and equal in size. For more durable connectors between knit conductive traces and wires, we used snap-buttons that we punched through the textile at one end of the knit traces. We created a simple visualization in Unity3D with the sensor data distorting a cylindric mesh using a custom vertex shader, to explore this input modality.

7 DISCUSSION

7.1 Manufacturing

Even though our work is framed in weft knitting, the basic concept of the presented sensor design is not limited to this technique; the principle idea of material arrangement is also viable for warp and/or circular knitting, however, the design possibilities are limited.

Weft knitting machines provide great flexibility and scalability, in the sense of agility in assembling fabrics. It enables to design multi-material composition on loop-level and therefore to install particular spaceR elements on specific locations with variable size, shape, and haptic characteristics, in a way that we cannot recognize in other knitting techniques. Although in this work we focused on a flat surrounding geometry for demonstrating the basic principle, our elements can be easily embedded in a variety of more complex shapes and patterns. Still, as the spaceR area itself occupies both needle beds, the options for designing knitting patterns on front and back faces as well as shaping it to a 3D-knit is limited on a two-bed machine, which is inherent to a spacer fabric structure. Embedding a spaceR into a tubular structure will also be challenging for the same reason, however, this is still possible on machines with more than two needle beds.

In terms of yarn handling, we recommend plating resistive yarn with the nylon, since both strands follow a more controlled path when compared to plying, where both strands are twisted together rather randomly. We furthermore found that tucking the filler at a few extra needles before inserting the first filler course is necessary to hold it in place, especially when the first course is a particularly short one, as is the case with our diamond-shaped rocker buttons, but also with the circular shapes. We refer to the Knitout files in the supplementary material for details.

7.2 Materials

Even though regular (full-area) spacer fabrics use spandex on both faces, we found it essential for our sensor regions to apply the spandex on the back face only. The contraction of the back face holds the tucked nylon in place and simultaneously causes its strands to erect. Increasing the loop size on the opposite face within the spacer region amplifies this structural imbalance. The nylon is thus enabled to move into its maximum upright position with a strong uni-directional tendency and creates a distinct bulge on the front face exclusively.

We would like to stress that we demonstrate a basic design principle for knitting a textile spacer button that can be further expanded; note that all materials used can be replaced by different ones, as long as they show the required basic functionality (i.e., the appropriate electrical and physical properties, respectively). In particular the decision for using a combination of two monofilament nylon strands for the filler is due to our subjective judgement. To our experience however, using single strands of equivalent volume (e.g., replacing the pair of ø=0.07 mm + ø=0.1 mm with a single ø=0.12 mm strand to achieve comparable filler volume) resulted in buttons that felt less compact and showed higher tendency to tilt sideways when pressed.

7.3 Sensing

We realize the resistance values of the samples presented in this work are rather high, however this is subject to the particular linear resistance of the resistive yarn we used, which is entirely replaceable, e.g., by the nylon-based F902 Merge A014[18], with only 3% of the P6204's average resistivity. The specified values still provide adequate delta to those of highly conductive yarn, which is required so the sensor is agnostic to actuation along the connectors to external electronics. We expect only the absolute resistance values to shift by a constant factor, yielding an equivalent dynamic range for precise sensing. Moreover, plating more resistive yarn into the filler could serve as an alternative to replacing the material, however this may cause interference with the filler strands at some point and could therefore affect the haptic qualities of the button.

In general, we acknowledge a low number of samples in our evaluation, we can therefore at this point make no statement about consistency between numerous makes of the same sensor type or sensor value drift over long periods of time and usage. Regarding short-term settling, we tested our baseline sensor with 20 N-actuation and observed the time it took for 5-second delta to *permanently* drop below 1% was 21.7 s. Over a 5-minute period at this actuation, we observed an accumulating resistance drop to 82.5% of the initial value. The reason for this is found in permanent geometric re-configuration of the internal structure, which is also reflected in the fact that the force required to keep the spacer at constant compression dropped by 9% during these 5 minutes, meaning that the spacer kept yielding. In between sensors, we noticed some minor variation and material-induced hysteresis due to filler relaxation. We furthermore tested our baseline sensor with forces up to 50 N and found that the sensitivity decreased with rising force, which was to be expected. In steps of 10 N, the relative change in resistance $\Delta R/R_0$ was -30%, -26%, -10%, -5%, and -3%, with R_0 being mean resistance at rest. Given relatively high settling effects and signal noise, we estimate measurements can be reasonably representative until up to ~30%, however this highly depends on the use case. More detailed evaluations would be required to make definite statements on sensitivity limits and noise.

While these properties are insufficient for precise measurement instruments, we do not see a crucial limitation for usage as an input device within the domain of HCI. For all of our applications, we could easily manage with slight modifications in data processing, straight-forward adaptive techniques, and quick calibration steps when switching between samples.

First washing tests were encouraging as they suggested the sensors are little susceptible to chemical and mechanical abrasion. Although the electrical properties change considerably at first, they quickly settle; furthermore, our sensors seem to be robust enough to endure several washing cycles without taking noticeable damage.

In terms of generalizability of our results, we expect the overall resistances of spaceR elements are subject to the ratio of width and height, i.e., resistance increases linearly with length and decreases inversely with width, as found by Ou et al. [35]. We did notice a constant dynamic range for all our tested diameters, however absolute resistance did change slightly with diameter. We attribute this to the placement of connectors, which does not account for this aspect, resulting in actual sensitive areas of different aspect ratios, which we approximate as 0.7, 1, and 1.13 for our variations with ø=17 mm, ø=25 mm, and ø=40 mm. We found the absolute resistance values indeed deviated by these factors, and as a result, we are confident that our results can be translated to sensors of different scales. For more details and actual data, we refer to the supplementary material.

[18] https://shakespeare-pf.com/product/nylon/

7.4 Design & Applications

We do see huge potential in incorporating spaceR sensors into 3D-knits, for drapable fabrics and fully-fashioned solutions, such as in sensory gloves or to equip actuators, similar to [27]. Note that the sensor is not exposed to considerable bending and stretching, when integrated in a 3D-knit that is shaped in unison to the draped object's geometry, hence its functionality is not restricted and its full dynamic range can still be harnessed.

For integration into a more complex knit, the layout of connector traces knit with conductive yarn will be more complex. These problems have been tackled and solved in the past, as demonstrated by the Bosch Sensor Glove, knitted with Stoll ADF (Autarc Direct Feeding) technology, although challenging from a knit engineering point of view. Furthermore, these solutions need to be tailored especially for the given product, we did therefore not investigate in this direction and focused on the sensor itself, where we still see much potential for further innovation. E.g., in terms of user interface expressiveness of our 4-way controller, one could imagine going beyond a simple 2-axis analog controller. Although not implemented, we envision input of temporal micro-gestures (e.g., performing semi-circular motions, left/right/up/down sequences, and combinations thereof), which could be easily detected with state-of-the art classification methods for triggering certain commands. From our experience with the already created spaceR device, we do not see substantial challenges in utilizing it for this and similar input modalities.

7.5 Lessons Learned

In the following, we summarize a number of insights that we find relevant for reproducing our spaceR elements.

- When bringing in new yarn during knitting, (e.g., conductive yarn for connecting traces), it is best not to start knitting within the fabric; instead, use two or three needles next to the knitted fabric to hold the new yarn in place and only drop those loops after several courses were knit. Otherwise, the cut ending may be pulled into the knit, causing severe fabrication flaws.
- When bringing in the nylon filler, also fix it with a few needles next to the spaceR element (cf. Knitout files in supplementary material). Especially when the first filler course is short (e.g., diamond shape, rocker-button) and filler spacing is high, the first u-turn of the nylon can otherwise lead to its escaping from the first tucked needles.
- For more complicated structures of multiple active regions (e.g., rocker-button, 4-way controller), it can be easier to not have the machine cut the resistive yarn in between regions. Holding it by several needles offside the fabric enables cutting it manually with scissors later on, which may be less of an effort than bringing the yarn in multiple times during knitting.
- To achieve good fabric shrinkage and therefore create a well-bulging spaceR, knit with half-gauge and use 100% spandex on the back face. Interlocking front and back faces at the element outline reinforces a distinct shape.
- Using low knitting speed for the nylon filler may lead to more consistent results.
- Use low stitch size to create round height profiles and high stitch size to create more edged profiles.
- To increase the spaceR elements' height, use high filler spacing and high stitch size for the front face, to facilitate rising of the nylon filaments, bulging out the front face structure.
- For multi-part elements, that need more than one pair of connecting traces (e.g, dip-button, 4-way controller), traces should be placed in a way that shorting has no effect, whenever possible. E.g., cf. Figure 15: when pins 1 and 4 are connected to ADCs, pins 2 and 3 can share one connection to ground (see the supplementary material for example schematics). Not only does this forgive accidental shorts between 2 and 3 in the knit, they can even be merged to a single knit trace, when this is required or less complex.
- When knitting connector traces, maximize the number of connecting loops between resistive and conductive yarns. Otherwise the connection may be erratic and cause noisy measurements, especially when the knit structure is moving and rearranging during actuation.

8 CONCLUSION & FUTURE WORK

We demonstrated a method for knitting compressible resistive sensors on flat-bed knitting machines. The resulting interface elements are highly expressive and versatile and can be fabricated ready-made, without requiring manual post-processing. They can be easily integrated into straightforward sensing environments, for reading continuous data with remarkable sensitivity. We reflected on design opportunities that provide good potential for designing for visual and tactile clues, enabling also eyes-free use case scenarios.

For future work, we plan to explore methods for improving layout of connector traces for simplifying arrangement of multiple elements on the textiles and for seamless incorporating them into fully-fashioned knitted solutions. Together with our partners in the knitting industry, we plan to dive deeper into topics of surface material characteristics in combinations with additional yarns and to unfold the full potential for designing sensor surfaces that are more complex in terms of visual and haptic appeal that could also provide additional means for communicating function. Furthermore, we plan to investigate the potential of so-called "soft spacer fabrics", where fluffy inlay is used to achieve an even softer and more comfortable appeal, closer to the character foams and pillows.

ACKNOWLEDGMENTS

Our thanks goes to Jim McCann and the CMU Textiles Lab for kindly providing their Knitout tools, and to Sara Mlakar of the Media Interaction Lab for her valuable input.

This research is part of the COMET project TextileUX (No. 865791, which is funded within the framework of COMET – Competence Centers for Excellent Technologies by BMVIT, BMDW, and the State of Upper Austria. The COMET program is handled by the FFG.

REFERENCES

[1] Roland Aigner, Andreas Pointner, Thomas Preindl, Rainer Danner, and Michael Haller. 2021. TexYZ: Embroidering Enameled Wires for Three Degree-of-Freedom Mutual Capacitive Sensing. In *Proceedings of the 2021 CHI Conference on Human Factors in Computing Systems (CHI '21).* Association for Computing Machinery,

New York, NY, USA, Article 499, 12 pages. DOI: http://dx.doi.org/10.1145/3411764.3445479

[2] Roland Aigner, Andreas Pointner, Thomas Preindl, Patrick Parzer, and Michael Haller. 2020. *Embroidered Resistive Pressure Sensors: A Novel Approach for Textile Interfaces.* Association for Computing Machinery, New York, NY, USA, 1–13. https://doi.org/10.1145/3313831.3376305

[3] Lea Albaugh, James McCann, Scott E. Hudson, and Lining Yao. 2021. Engineering Multifunctional Spacer Fabrics Through Machine Knitting. In *Proceedings of the 2021 CHI Conference on Human Factors in Computing Systems (CHI '21).* Association for Computing Machinery, New York, NY, USA, Article 498, 12 pages. DOI: http://dx.doi.org/10.1145/3411764.3445564

[4] Ozgur Atalay and William Richard Kennon. 2014. Knitted strain sensors: Impact of design parameters on sensing properties. *Sensors (Switzerland)* 14, 3 (2014), 4712–4730. DOI: http://dx.doi.org/10.3390/s140304712

[5] Natalija Baribina, Alexander Oks, Ilze Baltina, and Peteris Eizentals. 2018. Comparative analysis of knitted pressure sensors. *Engineering for Rural Development* 17 (2018), 1599–1604. DOI: http://dx.doi.org/10.22616/ERDev2018.17.N498

[6] Joran W. Booth, Dylan Shah, Jennifer C. Case, Edward L. White, Michelle C. Yuen, Olivier Cyr-Choiniere, and Rebecca Kramer-Bottiglio. 2018. OmniSkins: Robotic skins that turn inanimate objects into multifunctional robots. *Science Robotics* 3, 22 (2018), eaat1853. DOI: http://dx.doi.org/10.1126/scirobotics.aat1853

[7] Leah Buechley, Mike Eisenberg, Jaime Catchen, and Ali Crockett. 2008. The LilyPad Arduino: Using Computational Textiles to Investigate Engagement, Aesthetics, and Diversity in Computer Science Education. In *Proceedings of the SIGCHI Conference on Human Factors in Computing Systems (CHI '08).* Association for Computing Machinery, New York, NY, USA, 423–432. DOI: http://dx.doi.org/10.1145/1357054.1357123

[8] Shuwen Chen, Nan Wu, Shizhe Lin, Jiangjiang Duan, Zisheng Xu, Yuan Pan, Hongbo Zhang, Zheheng Xu, Liang Huang, Bin Hu, and Jun Zhou. 2020. Hierarchical elastomer tuned self-powered pressure sensor for wearable multifunctional cardiovascular electronics. *Nano Energy* 70 (2020), 104460. DOI: http://dx.doi.org/https://doi.org/10.1016/j.nanoen.2020.104460

[9] Jingyuan Cheng, Sundholm, Bo Zhou, Marco Hirsch, and Paul Lukowicz. 2016. Smart-surface: Large scale textile pressure sensors arrays for activity recognition. *Pervasive Mob. Comput.* 30 (2016), 97–112. DOI: http://dx.doi.org/10.1016/j.pmcj.2016.01.007

[10] Kyung Yun Choi, Jinmo Lee, Neska ElHaouij, Rosalind Picard, and Hiroshi Ishii. 2021a. *ASpire: Clippable, Mobile Pneumatic-Haptic Device for Breathing Rate Regulation via Personalizable Tactile Feedback.* Association for Computing Machinery, New York, NY, USA. https://doi.org/10.1145/3411763.3451602

[11] Minki Choi, Chi Cuong Vu, and Jooyong Kim. 2021b. Effects of Ag-coated twisted-yarns and equivalent circuits on textile pressure sensors. *Sensors and Actuators A: Physical* 332 (2021), 113150. DOI: http://dx.doi.org/https://doi.org/10.1016/j.sna.2021.113150

[12] Franklin N. Eventoff. 1983. Electronic pressure sensitive force transducer. (Oct. 1983). Patent No. US4489302A, Filed Sept. 24th., 1979, Issued March 15th., 1983.

[13] Sean Follmer, Daniel Leithinger, Alex Olwal, Nadia Cheng, and Hiroshi Ishii. 2012. *Jamming User Interfaces: Programmable Particle Stiffness and Sensing for Malleable and Shape-Changing Devices.* Association for Computing Machinery, New York, NY, USA, 519–528. https://doi.org/10.1145/2380116.2380181

[14] Jun Gong, Olivia Seow, Cedric Honnet, Jack Forman, and Stefanie Mueller. 2021. MetaSense: Integrating Sensing Capabilities into Mechanical Metamaterial. In *The 34th Annual ACM Symposium on User Interface Software and Technology (UIST '21).* Association for Computing Machinery, New York, NY, USA, 1063–1073. DOI: http://dx.doi.org/10.1145/3472749.3474806

[15] Jun Gong, Yu Wu, Lei Yan, Teddy Seyed, and Xing-Dong Yang. 2019. Tessutivo: Contextual Interactions on Interactive Fabrics with Inductive Sensing. In *Proceedings of the 32nd Annual ACM Symposium on User Interface Software and Technology (UIST '19).* Association for Computing Machinery, New York, NY, USA, 29–41. DOI: http://dx.doi.org/10.1145/3332165.3347897

[16] Paul Holleis, Albrecht Schmidt, Susanna Paasovaara, Arto Puikkonen, and Jonna Häkkilä. 2008. Evaluating Capacitive Touch Input on Clothes. In *Proceedings of the 10th International Conference on Human Computer Interaction with Mobile Devices and Services.* DOI: http://dx.doi.org/10.1145/1409240.1409250

[17] Cedric Honnet, Hannah Perner-Wilson, Marc Teyssier, Bruno Fruchard, Jürgen Steimle, Ana C. Baptista, and Paul Strohmeier. 2020. *PolySense: Augmenting Textiles with Electrical Functionality Using In-Situ Polymerization.* Association for Computing Machinery, New York, NY, USA, 1–13. https://doi.org/10.1145/3313831.3376841

[18] Hughes-Riley, Oliveira, and Dias. 2019. A Knitted Multi-Junction Pressure Sensor That Uses Electrical Resistance to Determine the Applied Pressure: Development and Characterization. *Proceedings* 32, 1 (2019), 3. DOI: http://dx.doi.org/10.3390/proceedings2019032003

[19] Alexandre Kaspar, Kui Wu, Yiyue Luo, Liane Makatura, and Wojciech Matusik. 2021. Knit Sketching: From Cut and Sew Patterns to Machine-Knit Garments. *ACM Trans. Graph.* 40, 4, Article 63 (July 2021), 15 pages. DOI: http://dx.doi.org/10.1145/3450626.3459752

[20] Ozgun Kilic Afsar, Ali Shtarbanov, Hila Mor, Ken Nakagaki, Jack Forman, Karen Modrei, Seung Hee Jeong, Klas Hjort, Kristina Höök, and Hiroshi Ishii. 2021. OmniFiber: Integrated Fluidic Fiber Actuators for Weaving Movement Based Interactions into the 'Fabric of Everyday Life'. In *The 34th Annual ACM Symposium on User Interface Software and Technology (UIST '21).* Association for Computing Machinery, New York, NY, USA, 1010–1026. DOI: http://dx.doi.org/10.1145/3472749.3474802

[21] Jin Hee (Heather) Kim, Shreyas Dilip Patil, Sarina Matson, Melissa Conroy, and Cindy Hsin-Liu Kao. 2022. KnitSkin: Machine-Knitted Scaled Skin for Locomotion. In *Proceedings of the 2022 CHI Conference on Human Factors in Computing Systems (CHI '22).* Association for Computing Machinery, New York, NY, USA, Article 391, 15 pages. DOI: http://dx.doi.org/10.1145/3491102.3502142

[22] Kyuyoung Kim, Jungrak Choi, Yongrok Jeong, Incheol Cho, Minseong Kim, Seunghwan Kim, Yongsuk Oh, and Inkyu Park. 2019a. Highly Sensitive and Wearable Liquid Metal-Based Pressure Sensor for Health Monitoring Applications: Integration of a 3D-Printed Microbump Array with the Microchannel. *Advanced Healthcare Materials* 8, 22 (2019), 1900978. DOI: http://dx.doi.org/https://doi.org/10.1002/adhm.201900978

[23] Kyungkwan Kim, Minhyun Jung, Sanghun Jeon, and Jihyun Bae. 2019b. Robust and scalable three-dimensional spacer textile pressure sensor for human motion detection. *Smart Materials and Structures* 28, 6 (may 2019), 065019. DOI: http://dx.doi.org/10.1088/1361-665x/ab1adf

[24] Seoktae Kim, Hyunjung Kim, Boram Lee, Tek-Jin Nam, and Woohun Lee. 2008. Inflatable Mouse: Volume-Adjustable Mouse with Air-Pressure-Sensitive Input and Haptic Feedback. In *Proceedings of the SIGCHI Conference on Human Factors in Computing Systems (CHI '08).* Association for Computing Machinery, New York, NY, USA, 211–224. DOI: http://dx.doi.org/10.1145/1357054.1357090

[25] Takuro Kuribara, Buntarou Shizuki, and Jiro Tanaka. 2013. Sinkpad: A Malleable Mouse Pad Consisted of an Elastic Material. In *CHI '13 Extended Abstracts on Human Factors in Computing Systems (CHI EA '13).* Association for Computing Machinery, New York, NY, USA, 1251–1256. DOI: http://dx.doi.org/10.1145/2468356.2468580

[26] Yiyue Luo, Yunzhu Li, Pratyusha Sharma, Wan Shou, Kui Wu, Michael Foshey, Beichen Li, Tomás Palacios, Antonio Torralba, and Wojciech Matusik. 2021. Learning human–environment interactions using conformal tactile textiles. *Nature Electronics* 4 (3 2021), 193–201.

[27] Yiyue Luo, Kui Wu, Andrew Spielberg, Michael Foshey, Tomas Palacios, Daniela Rus, and Wojciech Matusik. 2022. *Digital Fabrication of Pneumatic Actuators with Integrated Sensing by Machine Knitting.* Association for Computing Machinery, New York, NY, USA, to appear.

[28] James McCann. 2017. The Knitout (.k) File Format. (2017). https://textiles-lab.github.io/knitout/knitout.html

[29] James McCann, Lea Albaugh, Vidya Narayanan, April Grow, Wojciech Matusik, Jennifer Mankoff, and Jessica Hodgins. 2016. A Compiler for 3D Machine Knitting. *ACM Trans. Graph.* 35, 4, Article 49 (July 2016), 11 pages. DOI: http://dx.doi.org/10.1145/2897824.2925940

[30] Sara Mlakar, Mira Alida Haberfellner, Hans-Christian Jetter, and Michael Haller. 2021. Exploring Affordances of Surface Gestures on Textile User Interfaces. In *Designing Interactive Systems Conference 2021 (DIS '21).* Association for Computing Machinery, New York, NY, USA, 1159–1170. DOI: http://dx.doi.org/10.1145/3461778.3462139

[31] Sara Mlakar and Michael Haller. 2020. *Design Investigation of Embroidered Interactive Elements on Non-Wearable Textile Interfaces.* Association for Computing Machinery, New York, NY, USA, 1–10. https://doi.org/10.1145/3313831.3376692

[32] Vidya Narayanan, Lea Albaugh, Jessica Hodgins, Stelian Coros, and James McCann. 2018. Automatic Machine Knitting of 3D Meshes. *ACM Trans. Graph.* 37, 3, Article 35 (Aug. 2018), 15 pages. DOI: http://dx.doi.org/10.1145/3186265

[33] Alex Olwal, Jon Moeller, Greg Priest-Dorman, Thad Starner, and Ben Carroll. 2018. I/O Braid: Scalable Touch-Sensitive Lighted Cords Using Spiraling, Repeating Sensing Textiles and Fiber Optics. In *Proceedings of the 31st Annual ACM Symposium on User Interface Software and Technology (UIST '18).* Association for Computing Machinery, New York, NY, USA, 485–497. DOI: http://dx.doi.org/10.1145/3242587.3242638

[34] Maggie Orth, J. R. Smith, E. R. Post, J. A. Strickon, and E. B. Cooper. 1998. Musical Jacket. In *ACM SIGGRAPH 98 Electronic Art and Animation Catalog (SIGGRAPH '98).* Association for Computing Machinery, New York, NY, USA, 38. DOI: http://dx.doi.org/10.1145/281388.281456

[35] Jifei Ou, Daniel Oran, Don Derek Haddad, Joesph Paradiso, and Hiroshi Ishii. 2019. SensorKnit: Architecting Textile Sensors with Machine Knitting. *3D Printing and Additive Manufacturing* 6, 1 (2019), 1–11. DOI: http://dx.doi.org/10.1089/3dp.2018.0122

[36] Patrick Parzer, Adwait Sharma, Anita Vogl, Jürgen Steimle, Alex Olwal, and Michael Haller. 2017. SmartSleeve: Real-Time Sensing of Surface and Deformation Gestures on Flexible, Interactive Textiles, Using a Hybrid Gesture Detection Pipeline. In *Proceedings of the 30th Annual ACM Symposium on User Interface Software and Technology (UIST '17).* Association for Computing Machinery, New York, NY, USA, 565–577. DOI: http://dx.doi.org/10.1145/3126594.3126652

[37] E. R. Post, M. Orth, P. R. Russo, and N. Gershenfeld. 2000. E-broidery: Design and Fabrication of Textile-based Computing. *IBM Syst. J.* 39, 3-4 (July 2000), 840–860.

DOI: http://dx.doi.org/10.1147/sj.393.0840

[38] Ivan Poupyrev, Nan-Wei Gong, Shiho Fukuhara, Mustafa Emre Karagozler, Carsten Schwesig, and Karen E. Robinson. 2016. *Project Jacquard: Interactive Digital Textiles at Scale.* Association for Computing Machinery, New York, NY, USA, 4216–4227. https://doi.org/10.1145/2858036.2858176

[39] Mahsan Rofouei, Wenyao Xu, and Majid Sarrafzadeh. 2010. Computing with uncertainty in a smart textile surface for object recognition. In *2010 IEEE Conference on Multisensor Fusion and Integration*. 174–179. DOI: http://dx.doi.org/10.1109/MFI.2010.5604473

[40] Sigrid Rotzler, Christine Kallmayer, Christian Dils, Malte von Krshiwoblozki, Ulrich Bauer, and Martin Schneider-Ramelow. 2020. Improving the washability of smart textiles: influence of different washing conditions on textile integrated conductor tracks. *The Journal of The Textile Institute* 111, 12 (2020), 1766–1777. DOI: http://dx.doi.org/10.1080/00405000.2020.1729056

[41] Martin Schmitz, Jürgen Steimle, Jochen Huber, Niloofar Dezfuli, and Max Mühlhäuser. 2017. Flexibles: Deformation-Aware 3D-Printed Tangibles for Capacitive Touchscreens. In *Proceedings of the 2017 CHI Conference on Human Factors in Computing Systems (CHI '17)*. Association for Computing Machinery, New York, NY, USA, 1001–1014. DOI: http://dx.doi.org/10.1145/3025453.3025663

[42] A Schwarz-Pfeiffer, M Obermann, M O Weber, and A Ehrmann. 2016. Smarten up garments through knitting. *IOP Conference Series: Materials Science and Engineering* 141 (jul 2016), 012008. DOI: http://dx.doi.org/10.1088/1757-899x/141/1/012008

[43] Shayan Seyedin, Joselito M. Razal, Peter C. Innis, Ali Jeiranikhameneh, Stephen Beirne, and Gordon G. Wallace. 2015. Knitted Strain Sensor Textiles of Highly Conductive All-Polymeric Fibers. *ACS Applied Materials and Interfaces* 7, 38 (2015), 21150–21158. DOI: http://dx.doi.org/10.1021/acsami.5b04892

[44] Ronit Slyper, Ivan Poupyrev, and Jessica Hodgins. 2010. Sensing through Structure: Designing Soft Silicone Sensors. In *Proceedings of the Fifth International Conference on Tangible, Embedded, and Embodied Interaction (TEI '11)*. Association for Computing Machinery, New York, NY, USA, 213–220. DOI: http://dx.doi.org/10.1145/1935701.1935744

[45] David J. Spencer. 2001. *Knitting Technology: A Comprehensive Handbook and Practical Guide* (3 ed.). Woodhead Publishing.

[46] Paul Strohmeier, Jarrod Knibbe, Sebastian Boring, and Kasper Hornbæk. 2018. ZPatch: Hybrid Resistive/Capacitive ETextile Input *(TEI '18)*. Association for Computing Machinery, New York, NY, USA, 188–198. DOI: http://dx.doi.org/10.1145/3173225.3173242

[47] Mathias Sundholm, Jingyuan Cheng, Bo Zhou, Akash Sethi, and Paul Lukowicz. 2014. Smart-Mat: Recognizing and Counting Gym Exercises with Low-Cost Resistive Pressure Sensing Matrix *(UbiComp '14)*. Association for Computing Machinery, New York, NY, USA. DOI: http://dx.doi.org/10.1145/2632048.2636088

[48] Richard Vallett, Ryan Young, Chelsea Knittel, Youngmoo Kim, and Genevieve Dion. 2016. Development of a Carbon Fiber Knitted Capacitive Touch Sensor. *MRS Advances* 1, 38 (2016), 2641–2651. DOI: http://dx.doi.org/10.1557/adv.2016.498

[49] Anita Vogl, Patrick Parzer, Teo Babic, Joanne Leong, Alex Olwal, and Michael Haller. 2017. StretchEBand: Enabling Fabric-Based Interactions through Rapid Fabrication of Textile Stretch Sensors *(CHI '17)*. Association for Computing Machinery, New York, NY, USA, 2617–2627. DOI: http://dx.doi.org/10.1145/3025453.3025938

[50] Chi Cuong Vu and Jooyong Kim. 2020. Highly elastic capacitive pressure sensor based on smart textiles for full-range human motion monitoring. *Sensors and Actuators A: Physical* 314 (2020), 112029. DOI: http://dx.doi.org/https://doi.org/10.1016/j.sna.2020.112029

[51] Karsten Weiss and Heinz Wörn. 2005. The working principle of resistive tactile sensor cells. In *IEEE International Conference Mechatronics and Automation*. IEEE, 471–476. DOI: http://dx.doi.org/10.1109/ICMA.2005.1626593

[52] Irmandy Wicaksono and Joseph Paradiso. 2020. KnittedKeyboard: Digital Knitting of Electronic Textile Musical Controllers. In *Proceedings of the International Conference on New Interfaces for Musical Expression*, Romain Michon and Franziska Schroeder (Eds.). Birmingham City University, Birmingham, UK, 323–326. DOI: http://dx.doi.org/10.5281/zenodo.4813391

[53] Shanel Wu and Laura Devendorf. 2020. *Unfabricate: Designing Smart Textiles for Disassembly.* Association for Computing Machinery, New York, NY, USA, 1–14. https://doi.org/10.1145/3313831.3376227

[54] Wenyao Xu, Zhinan Li, Ming-Chun Huang, Navid Amini, and Majid Sarrafzadeh. 2011. eCushion: An eTextile Device for Sitting Posture Monitoring. In *2011 International Conference on Body Sensor Networks*. 194–199. DOI: http://dx.doi.org/10.1109/BSN.2011.24

[55] Tianhong Catherine Yu and James McCann. 2020. Coupling Programs and Visualization for Machine Knitting. In *Symposium on Computational Fabrication (SCF '20)*. Association for Computing Machinery, New York, NY, USA, Article 7, 10 pages. DOI: http://dx.doi.org/10.1145/3424630.3425410